Al-Gharabally and Almutairi *EURASIP Journal on Wireless Communications and Networking* (2019) 2019:78
https://doi.org/10.1186/s13638-019-1398-0

EURASIP Journal on Wireless Communications and Networking

RESEARCH Open Access

Frequency-domain subcarrier diversity receiver for discrete Hartley transform OFDM systems

Mishal Al-Gharabally and Ali F. Almutairi*

Abstract

In recent years, there has been an increasing interest in the use of the discrete Hartley transform (DHT) for orthogonal frequency-division multiplexing (OFDM). Previous studies have not reported an improvement in bit error rate (BER) when using a DHT-based OFDM without substantial complexity increase due to the fact that the DHT cannot diagonalize a circulant channel matrix but rather produces a unique structured matrix that has only a main diagonal and anti-diagonal. In this paper, the coupling between symmetric carriers is exploited by introducing a frequency-domain subcarrier diversity receiver for DHT-based OFDM systems. The proposed simple receiver structure takes advantage of the coupling to enhance the BER performance of the DHT-OFDM system by increasing the diversity gain between subcarriers. A detailed statistical and performance analysis of the system is presented, in which closed-form expressions of the average BER were derived. The proposed system performance was compared to the conventional discrete Fourier transform OFDM (DFT-OFDM), the generalized DHT-OFDM, and the DHT-precoded OFDM systems in terms of average BER and peak-to-average power ratio (PAPR). The proposed DHT-OFDM system outperforms the generalized DHT-OFDM system by 12 dB and outperforms the conventional DFT-OFDM and the DHT-precoded OFDM systems by 17 dB at an average BER of 10^{-5}. In terms of PAPR, the proposed DHT-OFDM system suffers from an approximately 5.5, 2, and 1 dB increase in PAPR when compared to the DHT-precoded OFDM, the conventional DFT-OFDM, and the generalized DHT-OFDM systems, respectively.

Keywords: Discrete hartley transform (DHT), Discrete fourier transform (DFT), Subcarrier coupling, Subcarrier diversity receiver, Peak-to-average power ratio (PAPR), OFDM

1 Introduction

Orthogonal frequency-division multiplexing (OFDM) is an attractive multicarrier modulation technique due to its robustness against the effects of multipath propagation such as intersymbol interference (ISI) and intercarrier interference (ICI), and hence, with the proper use of a cyclic prefix and the availability of channel state information, OFDM requires only simple one-tap equalization in the frequency-domain. In conventional OFDM systems, modulation, and demodulation of the orthogonal subcarriers are carried out using inverse discrete Fourier transform (IDFT) and discrete Fourier transform (DFT), respectively [1]. These operations are made fast and affordable due to the existence of many fast Fourier transform (FFT) and inverse fast Fourier transform (IFFT) algorithms as well as advances in field-programmable gate arrays (FPGA) [2–4].

Despite its many advantages, OFDM suffers from high peak-to-average power ratio (PAPR) which adds constraints on RF amplifiers and require them to operate in a very large linear region [5]. Furthermore, OFDM is also very sensitive to frequency offset and channel temporal variations that will affect the orthogonality between the subcarriers and causes ICI. Hence, OFDM systems require accurate synchronization between the transmitter and receiver [6–8], which may turn out to be a complicated task to achieve.

There is a great deal of work in the literature for ways to mitigate the above-mentioned impairments and improve the performance of OFDM systems. One such

*Correspondence: ali.almut@ku.edu.kw
Electrical Engineering Department, College of Engineering and Petroleum, Kuwait University, Kuwait, Kuwait

approach that picked up considerable attention in recent years is to replace or combine the DFT in conventional OFDM systems with other orthogonal transforms for the goal of improving system performance (reducing PAPR, minimizing bit error rate, etc.) or just simply reducing the computational complexity of the system. Examples of orthogonal transforms used to replace the DFT (or combined with DFT) are the discrete cosine transform (DCT) and discrete sine transform (DST) [9], the Walsh Hadamard transform (WHT) [10], the wavelet packet transform (WPT) [11], and the discrete Hartley transform (DHT) [12].

The DHT is a real-valued transform that requires only real arithmetic operations, which makes it appealing specifically for real-valued signals such as in binary phase shift keying (BPSK) modulations and optical communication systems [13]. In addition, the DHT and the inverse DHT (IDHT) have an identical kernel, which implies that the same circuitry can be used in both the transmitter and receiver. It will be shown later in this paper that the DHT also possesses some interesting properties that, if properly exploited, will lead to significant improvements in the system performance.

Several papers have considered replacing the DFT in conventional OFDM systems with DHT. The work in [9] considers replacing the DFT in an OFDM system with DCT, DST, and DHT, and investigates whether these transforms possess the same diagonalization property as the DFT (i.e., can these transform diagonalize circulant channel matrix in a similar way as the DFT). It was shown that unlike the DFT, the DHT cannot diagonalize a circulant channel matrix but, rather, produces a uniquely structured matrix that has only a main diagonal and an anti-diagonal. The work in [12] proposed using the IDHT and DHT for modulation and demodulation of OFDM systems. A relationship between the DFT kernel matrix and the DHT kernel matrix was presented and used to derive the input-output relation of the system in a way similar to that of the discrete Fourier transform OFDM (DFT-OFDM) system mathematically, which was then used to examine the system performance. Despite being simple and tractable, the approach in [12] did not show any improvement in performance of DHT-OFDM over DFT-OFDM, and hence, the only advantage is the reduction in computational complexity. Similar results were also reported in [13] for optical DHT-OFDM with no improvement in system performance over DFT-OFDM. In [14–16], the inability of the DHT to diagonalize the channel matrix was taken into consideration, and a transmitter/receiver architecture was devised to diagonalize the channel matrix. The devised system requires modification of both the transmitter and the receiver and is applied to quadrature amplitude modulation (QAM) signals where the IDHT/DHT is performed on both the inphase and the quadrature components of the QAM signal separately. The performance result shows that the proposed DHT-OFDM has the same performance as the DFT-OFDM. It was shown in [17] that in conventional DFT-OFDM systems, the transmitted symbols may not be accurately recovered when spectral nulls are present. To overcome the problem of spectral nulls in frequency-selective fading channels, the authors in [18] proposed a computationally efficient DHT-OFDM scheme using a one-level butterfly structure, and a simple single-tap equalizer can then be used to recover the transmitted symbols. The work in [19] exploits the fact that in DHT-OFDM, the channel matrix cannot be diagonalized. This unique structure of the resultant matrix implies that every two symmetric subcarriers are coupled together. A space frequency block-coded (SFBC) system with two antennas was proposed to exploit the frequency diversity inherited between every two coupled subcarriers, and a considerable improvement in performance was reported compared to DFT-OFDM at the price of increased complexity in the transmitter.

Instead of replacing DFT with DHT, the use of DHT in combination with DFT as a precoder or postcoder in OFDM systems was reported in [20–23]. The work in [20] and [21] considers using the DHT as a preceding block in OFDM systems to reduce PAPR. A DHT precoder is inserted before the IDFT at the transmitter, and an IDHT is inserted after the DFT at the receiver. Significant reductions in PAPR were reported compared to conventional DFT-OFDM systems. In [22], the authors considered DHT precoding in the transmitter. They prove that the DFT is the only transform that can enable single-tap equalization; in other words, DFT is the only transform that can diagonalize the channel matrix. The DHT and DFT are combined in a way that produces a sparse matrix for the combination. This condition facilitates single-tap equalization when a proper equalizer is used at the receiver. The proposed combined DHT-DFT exploits some of the diversity between the subcarriers, and hence, performance improvements in bit error rate (BER) were achieved. Finally, by combining DHT with DFT, the work in [23] introduced a new low-complexity transform named the **X**-transform. The new transform distributes each information symbol over all subcarriers, and combined with a minimum mean square error equalizer (MMSE), resulted in better diversity gains and BER.

2 Method

This paper investigates the performance of OFDM systems when the DFT in the conventional DFT-OFDM system is replaced by the DHT. To obtain an accurate understanding of the behavior of the proposed system, it is crucial to first develop a detailed mathematical model of the system and examine the effect of the wireless channel

on each subcarrier. The mathematical model revealed that when using the DHT instead of the DFT, the channel matrix is not diagonal and the subcarriers of the OFDM symbol are coupled together. The mathematical model also revealed that depending on the index of each subcarrier, different subarriers experience different levels of coupling interference (CI).

Instead of attempting to diagonalize the channel matrix and eliminate the coupling interference, this paper proposes a new detection scheme where the coupling between subcarriers is used to enhance the diversity gain and hence, improve the performance of the system. A detailed statistical analysis of the system is provided and new closed-form expressions of the average BER of the proposed DHT-OFDM system are derived.

The rest of this paper is organized as follows. Section 3 provides a detailed description of the DHT-OFDM system under consideration. In Section 4, we propose a simple detection scheme to exploit the diversity between subcarriers. A detailed statistical analysis of the parameters obtained in the previous section are presented in Section 5. In Section 6, closed-form expressions for the average BER of the system are derived. Simulation results are presented in Section 7, and 8 concludes this paper.

The following notations are used throughout the paper. Time-domain scalars are denoted in lowercase letters, while frequency-domain scalars are denoted in uppercase letters. Vectors and matrices are denoted in lowercase and uppercase bold, depending on whether they are time- or frequency-domain. $(.)^*$, $(.)^T$, and $(.)^H$ denote conjugation, transposition, and conjugate transpositions, respectively. N is the number of OFDM subcarriers, which is chosen to be a power of two, while n and k are the time index and the subcarrier index, respectively. The operator $E[.]$ denotes expectation.

3 System model

In this section, we provide a detailed review of the DHT-OFDM system under study. The analysis is carried out at the subcarrier level, and all of the mathematical expressions needed in later sections are derived and explained thoroughly.

Consider the baseband DHT-OFDM system depicted in Fig. 1. Since the DHT is a real-valued transform and takes real-value inputs; throughout this paper, we will assume that the baseband modulation used is BPSK, although it is possible to extend the system to higher-order complex modulations [16]. The output of the modulator in Fig. 1 is a sequence of BPSK data symbols $\{X(k)\}_{k=0}^{N-1}$ drawn from a set of finite alphabet $\left\{-\sqrt{E_b}, \sqrt{E_b}\right\}$, where E_b is the energy per bit. The data symbols are first converted into a parallel stream and then fed to the IDFT to modulate N orthogonal subcarriers. For convenience, analogously to the conventional DFT-OFDM, we will denote the input to the DHT as the time domain and the output as the frequency-domain. The output of the IDHT is the time-domain OFDM symbol $\{x(n)\}_{n=0}^{N-1}$, where $x(n)$ is given by

$$\begin{aligned} x(n) &= \mathrm{IDHT}\{X(k)\} \\ &= \frac{1}{\sqrt{N}} \sum_{k=0}^{N-1} X(k)\, \mathrm{cas}\left(\frac{2\pi nk}{N}\right). \end{aligned} \tag{1}$$

The function $\mathrm{cas}(\nu)$ in (1) is the Hartley transform kernel and is given by $\mathrm{cas}(\nu) = \cos(\nu) + \sin(\nu)$. One of the advantages of the Hartley transform is that it has the same

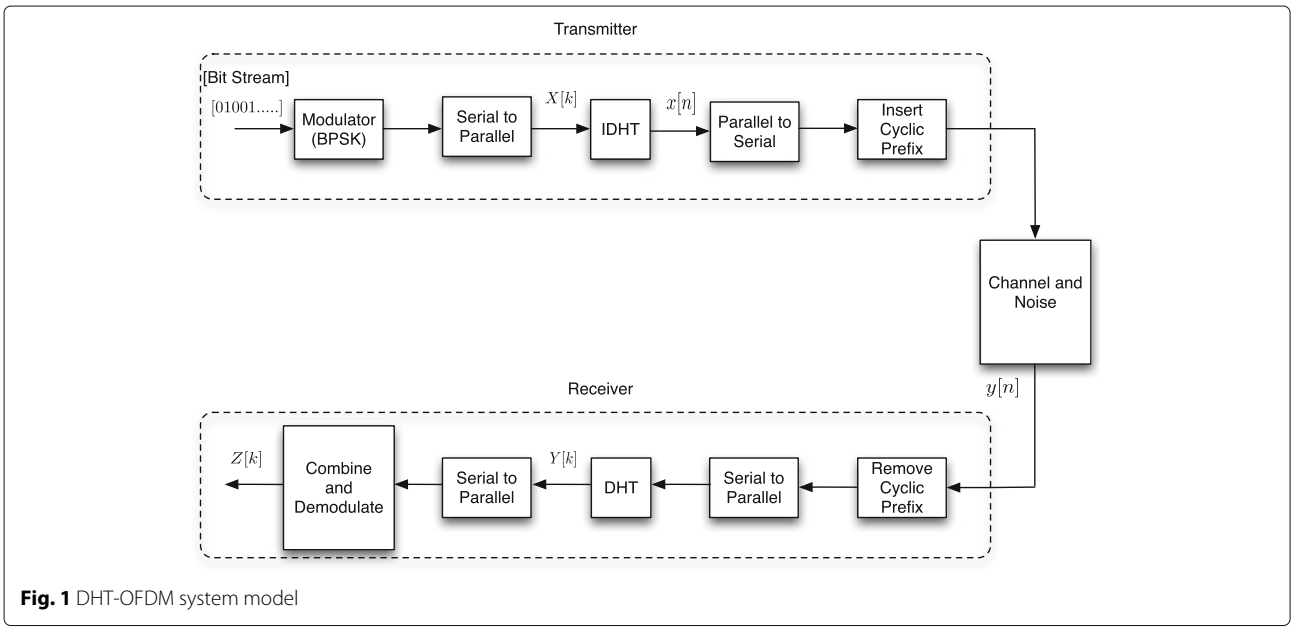

Fig. 1 DHT-OFDM system model

kernel for DHT and IDHT [24]; that is, the DHT of $x(n)$ is given by

$$\begin{aligned} X(k) &= \mathrm{DHT}\{x(n)\} \\ &= \frac{1}{\sqrt{N}} \sum_{n=0}^{N-1} x(n) \,\mathrm{cas}\left(\frac{2\pi nk}{N}\right). \end{aligned} \tag{2}$$

A cyclic prefix with a length longer than the maximum delay spread of the multipath channel is added to the OFDM symbol in (1) to eliminate ISI. The received OFDM symbol is then given by the following convolution sum:

$$y(n) = \sum_{l=0}^{L-1} h(l)\, x(n-l) + w(n) \tag{3}$$

where $w(n)$ is AWGN with zero mean and variance $\sigma_w^2 = N_o$, and $h(l)$ is the lth tap of the channel impulse response. We assume that the channel has a total of L taps and is wide sense stationary uncorrelated scattering (WSSUS). Expressing $x(n-l)$ in (3) in terms of its DHT by using the shift property of the Hartley transform [25], namely, as

$$x(n-n_o) \longleftrightarrow X(k)\cos\left(\frac{2\pi n_o k}{N}\right) + X(N-k)\sin\left(\frac{2\pi n_o k}{N}\right) \tag{4}$$

we can rewrite $y(n)$ in (3) as follows:

$$\begin{aligned} y(n) = \sum_{l=0}^{L-1} h(l)\, \frac{1}{\sqrt{N}} \sum_{k=0}^{N-1} &\left\{ X(k)\cos\left(\frac{2\pi lk}{N}\right) \right. \\ &\left. + X(N-k)\sin\left(\frac{2\pi lk}{N}\right) \right\} \mathrm{cas}\left(\frac{2\pi nk}{N}\right) + w(n) \end{aligned} \tag{5}$$

where $X(k)$ and $X(N-k)$ are obtained from (2). At the receiver, the received signal in (5) is passed through the DHT, and the frequency-domain received symbol at the kth subcarrier is produced as shown below:

$$\begin{aligned} Y(k) &= \frac{1}{\sqrt{N}} \sum_{n=0}^{N-1} y(n) \mathrm{cas}\left(\frac{2\pi nk}{N}\right) \\ &= \left(\sum_{n=0}^{N-1} \sum_{l=0}^{L-1} h(l)\, \frac{1}{N} \sum_{k=0}^{N-1} \left\{ X(k)\cos\left(\frac{2\pi lk}{N}\right) + X(N-k)\sin\left(\frac{2\pi lk}{N}\right) \right\} \right. \\ &\quad \left. \times \mathrm{cas}^2\left(\frac{2\pi nk}{N}\right) \right) + \frac{1}{\sqrt{N}} \sum_{n=0}^{N-1} w(n) \mathrm{cas}\left(\frac{2\pi nk}{N}\right). \end{aligned} \tag{6}$$

At this stage, we can further manipulate (6) by dividing the expression into two terms, namely, the desired subcarrier k term and a term involving all other subcarriers $i \neq k$. The received OFDM symbol at the kth subcarrier will then be expressed as

$$\begin{aligned} Y(k) = &\sum_{n=0}^{N-1} \sum_{l=0}^{L-1} h(l)\, \frac{1}{N} \left\{ X(k)\cos\left(\frac{2\pi lk}{N}\right) \right. \\ &\left. + X(N-k)\sin\left(\frac{2\pi lk}{N}\right) \right\} \mathrm{cas}^2\left(\frac{2\pi nk}{N}\right) \\ &+ \sum_{n=0}^{N-1} \sum_{l=0}^{L-1} h(l)\, \frac{1}{N} \sum_{i=0, i\neq k}^{N-1} \left\{ X(i)\cos\left(\frac{2\pi li}{N}\right) \right. \\ &\left. + X(N-i)\sin\left(\frac{2\pi li}{N}\right) \right\} \mathrm{cas}\left(\frac{2\pi ni}{N}\right) \mathrm{cas}\left(\frac{2\pi nk}{N}\right) \\ &+ \frac{1}{\sqrt{N}} \sum_{n=0}^{N-1} w(n) \mathrm{cas}\left(\frac{2\pi nk}{N}\right). \end{aligned} \tag{7}$$

The received symbol (7) now consists of three terms and can be written as $Y(k) = D(k) + I(k) + W(k)$, where

$$\begin{aligned} D(k) = \sum_{n=0}^{N-1} \sum_{l=0}^{L-1} h(l)\, \frac{1}{N} &\left\{ X(k)\cos\left(\frac{2\pi lk}{N}\right) \right. \\ &\left. + X(N-k)\sin\left(\frac{2\pi lk}{N}\right) \right\} \mathrm{cas}^2\left(\frac{2\pi nk}{N}\right) \end{aligned} \tag{8}$$

is the received OFDM symbol at the desired subcarrier k, and

$$\begin{aligned} I(k) = \sum_{n=0}^{N-1} \sum_{l=0}^{L-1} h(l)\, \frac{1}{N} \sum_{i=0, i\neq k}^{N-1} &\left\{ X(i)\cos\left(\frac{2\pi li}{N}\right) \right. \\ &\left. + X(N-i)\sin\left(\frac{2\pi li}{N}\right) \right\} \mathrm{cas}\left(\frac{2\pi ni}{N}\right) \mathrm{cas}\left(\frac{2\pi nk}{N}\right) \end{aligned} \tag{9}$$

is the contribution of all other subcarriers to subcarrier k, which is also known in literature as ICI, and $W(k)$ is the DHT of the additive noise. Let us start by looking at the ICI term $I(k)$. By invoking the orthogonality property of the cas function [26], namely,

$$\frac{1}{N} \sum_{n=0}^{N-1} \mathrm{cas}\left(\frac{2\pi ni}{N}\right) \mathrm{cas}\left(\frac{2\pi nk}{N}\right) = \begin{cases} 1 & \text{if } i = k \\ 0 & \text{if } i \neq k \end{cases} \tag{10}$$

we can easily see that the ICI term $I(k)$ in (9) vanishes to zero. This is not true if the channel is time varying, and if that is the case, the ICI will be present and will greatly degrade the system performance if not compensated for. It can be seen from (10) that the desired term $D(k)$ can be simplified to

$$\begin{aligned} D(k) = &\sum_{l=0}^{L-1} h(l)\, X(k)\cos\left(\frac{2\pi lk}{N}\right) \\ &+ \sum_{l=0}^{L-1} h(l)\, X(N-k)\sin\left(\frac{2\pi lk}{N}\right). \end{aligned} \tag{11}$$

Now let

$$\alpha(k) = \sum_{l=0}^{L-1} h(l) \cos\left(\frac{2\pi lk}{N}\right) \tag{12}$$

$$\beta(k) = \sum_{l=0}^{L-1} h(l) \sin\left(\frac{2\pi lk}{N}\right). \tag{13}$$

We can write $D(k)$ in the following convenient form:

$$D(k) = \alpha(k)X(k) + \beta(k)X(N-k) \tag{14}$$

We observe at this point that every subcarrier k (except for $k = 0$ and $k = N/2$) is coupled with subcarrier $N-k$. Coupling between subcarriers degrades system performance, and we will hereafter denote the term involving $\beta(k)$ in (14) as coupling interference (CI). Finally, the received OFDM symbol after DHT is given by

$$Y(k) = \alpha(k)X(k) + \beta(k)X(N-k) + W(k). \tag{15}$$

4 Detection

4.1 Observations

Before exploiting the advantages of DHT and explaining the proposed detection scheme, we first list the following observations:

1 For subcarrier $k = 0$:

$$\alpha(0) = \sum_{l=0}^{L-1} h_l, \qquad \beta(0) = 0$$

and hence,

$$Y(0) = \alpha(0)X(0) + W(0).$$

2 For subcarrier $k = N/2$:

$$\alpha(N/2) = \sum_{l=0}^{L-1} h_l \cos(\pi l), \qquad \beta(N/2) = 0$$

and hence,

$$Y(N/2) = \alpha(N/2)X(N/2) + W(N/2).$$

We see from the above observations that subcarriers 0 and $N/2$ are not coupled with any other subcarrier; therefore, there will be no CI. The detection of data symbols on subcarriers 0 and $N/2$ is fairly simple and can be done using a one-tap frequency-domain equalizer, assuming channel state information is available at the receiver. Further, we also raise the following important observation for all subcarriers $k \neq 0, N/2$:

3 For subcarrier $k = N - k$:

$$\alpha(N-k) = \sum_{l=0}^{L-1} h(l) \cos\left(\frac{2\pi l(N-k)}{N}\right)$$

$$\beta(N-k) = \sum_{l=0}^{L-1} h(l) \sin\left(\frac{2\pi l(N-k)}{N}\right)$$

and by simple trigonometric manipulation, we see that

$$\alpha(N-k) = \alpha(k)$$
$$\beta(N-k) = -\beta(k).$$

We see from the third observation above that there is a relation between the channel gains of the coupled subcarriers k and $N-k$. This relation will be exploited to design a simple detection scheme that can decouple the two subcarriers and provide superior BER performance compared to the conventional DFT-OFDM system.

4.2 Detection scheme

From the observations presented above, the coupling between subcarriers may be viewed as one of the disadvantages of using the DHT with OFDM and will greatly reduce the performance of DHT-OFDM systems if not dealt with. If the coupling between subcarriers is treated as interference, then it will have the same effect on performance as ICI and will produce an irreducible error floor in the average BER of the system. Instead of treating the coupling between subcarriers as a source of performance degradation, we will present a simple combining receiver that will take advantage of the coupling and use it to enhance the performance of the system by increasing the diversity gain between subcarriers. The proposed scheme is concerned with the decoupling and detection of all subcarriers $k \neq 0, N/2$. For subcarriers $k = 0, N/2$, the detection is fairly simple, as mentioned above. A block diagram of the proposed detection scheme is shown in Fig. 2.

Consider first combining every two coupled subcarriers together to form the vector

$$\tilde{\mathbf{Y}} = \begin{bmatrix} Y(k) & -Y^*(N-k) \end{bmatrix}^T. \tag{16}$$

Using (15), we can write $\tilde{\mathbf{Y}}$ as

$$\begin{bmatrix} Y(k) \\ -Y^*(N-k) \end{bmatrix} = \begin{bmatrix} \alpha(k) & \beta(k) \\ -\beta^*(N-k) & -\alpha^*(N-k) \end{bmatrix} \begin{bmatrix} X(k) \\ X(N-k) \end{bmatrix} + \begin{bmatrix} W(k) \\ -W^*(N-k) \end{bmatrix}. \tag{17}$$

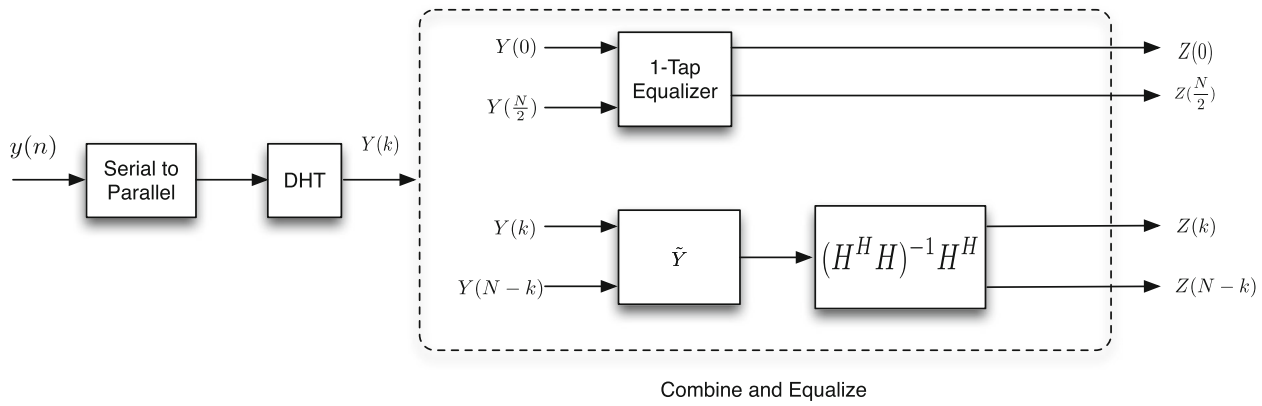

Fig. 2 Proposed detection scheme

Making use of the third observation, the vector $\tilde{\mathbf{Y}}$ in (17) then becomes

$$\begin{bmatrix} Y(k) \\ -Y^*(N-k) \end{bmatrix} = \begin{bmatrix} \alpha(k) & \beta(k) \\ \beta^*(k) & -\alpha^*(k) \end{bmatrix} \begin{bmatrix} X(k) \\ X(N-k) \end{bmatrix} + \begin{bmatrix} W(k) \\ -W^*(N-k) \end{bmatrix}$$

$$\tilde{\mathbf{Y}} = \mathbf{H}\mathbf{X} + \mathbf{W} \tag{18}$$

where

$$\mathbf{H} = \begin{bmatrix} \alpha(k) & \beta(k) \\ \beta^*(k) & -\alpha^*(k) \end{bmatrix} \tag{19}$$

$$\mathbf{X} = [X(k) \;\; X(N-k)]^T \tag{20}$$

$$\mathbf{W} = \left[W(k) \;\; -W^*(N-k)\right]^T. \tag{21}$$

We observe at this point that by combining every two coupled subcarriers k and $N-k$ using (16), the channel matrix $\mathbf{H}$ in (18) now has a form similar to that of the Alamouti dual transmit diversity channel matrix. Multiplying $\tilde{\mathbf{Y}}$ in (18) by the pseudo-inverse of $\mathbf{H}$, that is, $(\mathbf{H}^H\mathbf{H})^{-1}\mathbf{H}^H$ we get

$$\begin{aligned} \mathbf{Z} &= (\mathbf{H}^H\mathbf{H})^{-1}\mathbf{H}^H\tilde{\mathbf{Y}} \\ &= \mathbf{X} + \tilde{\mathbf{W}} \end{aligned} \tag{22}$$

where

$$\mathbf{Z} = [Z(k) \;\; Z(N-k)]^T \tag{23}$$

$$\tilde{\mathbf{W}} = (\mathbf{H}^H\mathbf{H})^{-1}\mathbf{H}^H\mathbf{W} = \left[\tilde{W}(k) \;\; \tilde{W}(N-k)\right]^T. \tag{24}$$

Based on the above equations, we can see that on the subcarrier level, the equalized output of the two coupled subcarriers are

$$Z(k) = X(k) + \tilde{W}(k) \tag{25}$$

$$Z(N-k) = X(N-k) + \tilde{W}(N-k). \tag{26}$$

Clearly, the two subcarriers k and $N-k$ are now completely decoupled.

5 Statistical analysis

In this section, we provide a detailed statistical analysis for some of the parameters that are derived in the previous sections and will be used in Section 6 to obtain closed-form expressions for the error probability. The noise term in (25) is given by

$$\tilde{W}(k) = \frac{\alpha^*(k)W(k) - \beta(k)W^*(N-k)}{|\alpha(k)|^2 + |\beta(k)|^2} \tag{27}$$

which is clearly complex Gaussian with zero mean and variance equal to

$$\sigma^2_{\tilde{W}} = E\left[|\tilde{W}(k)|^2\right] = \frac{N_o}{|\alpha|^2 + |\beta|^2} \tag{28}$$

where we have assumed that the variance of $W(k)$ is N_o. It can be shown that the variance of $\tilde{W}(N-k)$ is equal to the variance of $\tilde{W}(k)$.

The parameter $\alpha(k)$ in (12) is zero mean with variance

$$\begin{aligned} \sigma^2_{\alpha(k)} &= E[\,|\alpha(k)|^2] \\ &= E\left[\sum_{l=0}^{L-1}\sum_{m=0}^{L-1} h(l)h^*(m)\cos\left(\frac{2\pi lk}{N}\right)\cos\left(\frac{2\pi mk}{N}\right)\right] \\ &= \left[\sum_{l=0}^{L-1}\sum_{m=0}^{L-1} J_o(2\pi f_d T)\sigma^2_{h(l)}\delta(l-m)\cos\left(\frac{2\pi lk}{N}\right)\cos\left(\frac{2\pi mk}{N}\right)\right] \end{aligned} \tag{29}$$

where $J_o(\cdot)$ is the 0th order Bessel function of the first kind, f_d is the maximum Doppler frequency, T is the data symbol period, and $\sigma^2_{h(l)}$ is the variance of $h(l)$. If the

channel is assumed to be constant during an entire OFDM symbol then $f_d = 0$ and (29) reduces to

$$\sigma^2_{\alpha(k)} = \sum_{l=0}^{L-1} \sigma^2_{h(l)} \cos^2\left(\frac{2\pi lk}{N}\right) = \frac{1}{2}\sum_{l=0}^{L-1} \sigma^2_{h(l)} + \frac{1}{2}\sum_{l=0}^{L-1} \sigma^2_{h(l)} \cos\left(\frac{4\pi lk}{N}\right). \quad (30)$$

In a similar way, the variance of $\beta(k)$ is

$$\sigma^2_{\beta(k)} = \frac{1}{2}\sum_{l=0}^{L-1} \sigma^2_{h(l)} - \frac{1}{2}\sum_{l=0}^{L-1} \sigma^2_{h(l)} \cos\left(\frac{4\pi lk}{N}\right). \quad (31)$$

An interesting observation here is that not all of the N subcarriers in an OFDM symbol will experience the same variance of $\alpha(k)$ and $\beta(k)$. We can divide the N subcarriers into three different groups depending on $\sigma^2_{\alpha(k)}$ and $\sigma^2_{\beta(k)}$. This will also enable us to analyze the performance of the subcarriers individually.

Group 1: This case contains all subcarriers with $\sigma^2_{\beta(k)} = 0$. Looking at (30) and (31), we observe that for subcarriers $k = 0$ and $k = N/2$, the variance $\sigma^2_{\alpha(0)} = \sigma^2_{\alpha(N/2)} = \sum_{l=0}^{L-1} \sigma^2_{h(l)}$ and $\sigma^2_{\beta(0)} = \sigma^2_{\beta(N/2)} = 0$. This also falls in line with the previous results obtained in (13). It is also important to mention here that for $k = 0$ and $k = N/2$, the expression for the received signal in (15) reduces to

$$Y(k) = \alpha(k)X(k) + W(k) \quad (32)$$

which is identical to the received signal in the conventional DFT-OFDM system, and hence, the performance of these two subcarriers will be used as a benchmark to gauge any performance improvement obtained by the proposed DHT-OFDM system.

Group 2: If the term $\cos(4\pi lk/N)$ is equal to zero in (30) and (31), both the variances of $\alpha(k)$ and $\beta(k)$ are equal to $\sigma^2_{\alpha(k)} = \sigma^2_{\beta(k)} = \frac{1}{2}\sum_{l=0}^{L-1} \sigma^2_{h(l)}$. For example, if $N = 64$ and $L = 7$, then for subcarriers $k = (8, 24, 40, 56)$, the variances $\sigma^2_{\alpha(k)}$ and $\sigma^2_{\beta(k)}$ are equal.

Group 3: For all other subcarriers not belonging to any of the two groups above, the variances $\sigma^2_{\alpha(k)}$ and $\sigma^2_{\beta(k)}$ are not equal and are given in (30) and (31).

6 Performance analysis

In this section, we derive closed-form expressions for the average BER corresponding to each group of subcarriers, as mentioned in Section 5.

6.1 Group 1

($\sigma^2_\beta = 0$): This case contains two subcarriers $k = 0$ and $k = N/2$. From (15), we can see that the received signal after DHT is given by

$$Y(0) = \alpha(0)X(0) + W(0). \quad (33)$$

The equalized signal $Z(0)$ using a one-tap frequency-domain equalizer for subcarrier $k = 0$ is given by

$$Z(0) = \frac{Y(0)\alpha^*(0)}{|\alpha(0)|^2} = X(0) + \frac{W(0)\alpha^*(0)}{|\alpha(0)|^2} \quad (34)$$

conditioned on $\alpha(0)$, the noise in (34) is complex Gaussian with zero mean and variance equal to $\frac{N_o}{2|\alpha(0)|^2}$ per dimension. The instantaneous BER for subcarrier $k = 0$ is then given by

$$P_{e1} = Pr\left(Re\{Z(0)\} < 0 | X(0) = \sqrt{E_b}\right) = Q\left(\sqrt{2\gamma_1}\right) \quad (35)$$

where $Re\{Z(0)\}$ denotes the real part of $Z(0)$ and

$$\gamma_1 = \frac{E_b}{N_o}|\alpha(0)|^2 \quad (36)$$

is an exponential random variable with a probability density function equal to

$$f_{\gamma_1}(\gamma_1) = \frac{1}{\bar{\gamma_1}} e^{-\frac{\gamma_1}{\bar{\gamma_1}}} \quad (37)$$

and

$$\bar{\gamma_1} = \frac{2E_b}{N_o}\sigma^2_{\alpha(0)}. \quad (38)$$

The average BER is then calculated by averaging (35) over all values of γ_1 which can be shown to be equal to [27]

$$\bar{P_{e1}} = \int_0^\infty Q\left(\sqrt{2\gamma_1}\right) \cdot \frac{1}{\bar{\gamma_1}} e^{-\frac{\gamma_1}{\bar{\gamma_1}}} d\gamma_1 = \frac{1}{2}\left(1 - \sqrt{\frac{\bar{\gamma_1}}{1+\bar{\gamma_1}}}\right) = \frac{1}{2}\left(1 - \sqrt{\frac{\frac{2E_b}{N_o}\sigma^2_\alpha(0)}{1+\frac{2E_b}{N_o}\sigma^2_\alpha(0)}}\right) = \frac{1}{2}\left(1 - \sqrt{\frac{\frac{2E_b}{N_o}\sum_{l=0}^{L-1}\sigma^2_h(l)}{1+\frac{2E_b}{N_o}\sum_{l=0}^{L-1}\sigma^2_h(l)}}\right). \quad (39)$$

The average BER for $k = N/2$ can be shown to be equal the average BER for subcarrier $k = 0$.

6.2 Group 2

$\left(\sigma^2_{\alpha(k)} = \sigma^2_{\beta(k)}\right)$: This case corresponds to subcarriers k where the variances of $\alpha(k)$ and $\beta(k)$ are equal. The equalized signal at the kth subcarrier is given by (25)

$$Z(k) = X(k) + \tilde{W}(k) \quad (40)$$

where the noise term is shown in (27), and its variance is given in (28). The instantaneous BER is

$$P_{e2} = Pr\left(Re\{Z(k)\} < 0 | X(k) = \sqrt{E_b}\right) = Q\left(\sqrt{\frac{2E_b(|\alpha(k)|^2 + |\beta(k)|^2)}{N_o}}\right) \quad (41)$$

The term $\left(|\alpha(k)|^2+|\beta(k)|^2\right)$ in (41) is chi-square distributed with 4 degrees of freedom. Define the variable λ_2 as

$$\lambda_2 = |\alpha(k)|^2 + |\beta(k)|^2 \tag{42}$$

with density function

$$f_{\lambda_2}(\lambda_2) = \frac{1}{4\sigma^4}\lambda_2 e^{-\frac{\lambda_2}{2\sigma^2}} \tag{43}$$

where $\sigma^2 = \frac{1}{2}\sigma^2_{\alpha(k)} = \frac{1}{2}\sigma^2_{\beta(k)}$. Let

$$\gamma_2 = \frac{E_b}{N_o}\lambda_2. \tag{44}$$

The density function of γ_2 is obtained by [28]

$$\begin{aligned} f_{\gamma_2}(\gamma_2) &= \frac{N_o}{E_b} f_{\lambda_2}\left(\frac{N_o}{E_b}\gamma_2\right) \\ &= \frac{\left(\frac{N_o}{E_b}\right)^2}{4\sigma^4}\gamma_2 e^{-\frac{N_o\gamma_2}{2E_b\sigma^2}} = \frac{1}{\bar{\gamma_2}^2}\gamma_2 e^{-\frac{\gamma_2}{\bar{\gamma_2}}} \end{aligned} \tag{45}$$

where $\bar{\gamma_2} = \frac{2E_b\sigma^2}{N_o}$. The average BER is then obtained from [27]

$$\begin{aligned} \bar{P_{e2}} &= \int_0^\infty Q\left(\sqrt{2\gamma_2}\right)\cdot\frac{1}{\bar{\gamma_2}^2}\gamma_2 e^{-\frac{\gamma_2}{\bar{\gamma_2}}}d\gamma_2 \\ &= \left(\frac{1-\mu}{2}\right)^2(2+\mu) \end{aligned} \tag{46}$$

where $\mu = \sqrt{\frac{\bar{\gamma_2}}{1+\bar{\gamma_2}}} = \sqrt{\frac{\frac{1}{2}\frac{E_b}{N_o}\sum_{l=0}^{L-1}\sigma^2_{h(l)}}{1+\frac{1}{2}\frac{E_b}{N_o}\sum_{l=0}^{L-1}\sigma^2_{h(l)}}}$.

6.3 Group 3

$\left(\sigma^2_{\alpha(k)} \neq \sigma^2_{\beta(k)}\right)$: Following along the same steps of case 2, the instantaneous BER for the case when $\sigma^2_\alpha \neq \sigma^2_\beta$ is given by (41)

$$P_{e_3} = Q\left(\sqrt{\frac{2E_b(|\alpha(k)|^2+|\beta(k)|^2)}{N_o}}\right). \tag{47}$$

Let $\lambda_3 = |\alpha(k)|^2 + |\beta(k)|^2$. The density function of λ_3 is [28, 29]

$$\begin{aligned} f_{\lambda_3}(\lambda_3) &= \frac{\lambda_{\beta(k)}}{\lambda_{\beta(k)}-\lambda_{\alpha(k)}}\lambda_{\alpha(k)}e^{-\lambda_{\alpha(k)}\lambda_3} \\ &\quad + \frac{\lambda_{\alpha(k)}}{\lambda_{\alpha(k)}-\lambda_{\beta(k)}}\lambda_{\beta(k)}e^{-\lambda_{\beta(k)}\lambda_3} \\ &= A_1\lambda_{\alpha(k)}e^{-\lambda_{\alpha(k)}\lambda_3} + A_2\lambda_{\beta(k)}e^{-\lambda_{\beta(k)}\lambda_3} \end{aligned} \tag{48}$$

where

$$A_1 = \frac{\lambda_{\beta(k)}}{\lambda_{\beta(k)}-\lambda_{\alpha(k)}} \tag{49}$$

$$A_2 = \frac{\lambda_{\alpha(k)}}{\lambda_{\alpha(k)}-\lambda_{\beta(k)}} \tag{50}$$

with $\lambda_{\alpha(k)} = 1/\sigma^2_{\alpha(k)}$ and $\lambda_{\beta(k)} = 1/\sigma^2_{\beta(k)}$.

Let $\gamma_3 = \frac{E_b}{N_o}\lambda_3$; then, similar to (45), the density function of γ_3 becomes

$$f_{\gamma_3}(\gamma_3) = \frac{A_1}{\bar{\gamma_\alpha}}e^{-\frac{\gamma_3}{\bar{\gamma_\alpha}}} + \frac{A_2}{\bar{\gamma_\beta}}e^{-\frac{\gamma_3}{\bar{\gamma_\beta}}} \tag{51}$$

where $\bar{\gamma_\alpha} = \frac{E_b}{N_o}\sigma^2_{\alpha(k)}$ and $\bar{\gamma_\beta} = \frac{E_b}{N_o}\sigma^2_{\beta(k)}$. Finally, the average BER for case 3 is obtained by

$$\begin{aligned} \bar{P}_{e_3} &= \int_0^\infty Q\left(\sqrt{2\gamma_3}\right)\cdot f_{\gamma_3}(\gamma_3)d\gamma_3 \\ &= A_1\int_0^\infty Q\left(\sqrt{2\gamma_3}\right)\cdot\frac{1}{\bar{\gamma_\alpha}}e^{-\frac{\gamma_3}{\bar{\gamma_\alpha}}}d\gamma_3 \\ &\quad + A_2\int_0^\infty Q\left(\sqrt{2\gamma_3}\right)\cdot\frac{1}{\bar{\gamma_\beta}}e^{-\frac{\gamma_3}{\bar{\gamma_\beta}}}d\gamma_3 \\ &= \frac{A_1}{2}\left(1-\sqrt{\frac{\frac{E_b}{N_o}\sigma^2_{\alpha(k)}}{1+\frac{E_b}{N_o}\sigma^2_{\alpha(k)}}}\right) \\ &\quad + \frac{A_2}{2}\left(1-\sqrt{\frac{\frac{E_b}{N_o}\sigma^2_{\beta(k)}}{1+\frac{E_b}{N_o}\sigma^2_{\beta(k)}}}\right) \end{aligned} \tag{52}$$

where $\sigma^2_{\alpha(k)}$ and $\sigma^2_{\beta(k)}$ in (52) are given in (30) and (31), respectively.

7 Numerical results

In this section, simulations are conducted to confirm the theoretical analysis presented in Section 6. The simulation parameters are listed in Table 1. Each OFDM symbol consists of 64 or 256 subcarriers; all subcarriers are utilized for data transmission, and the data modulation used is BPSK. No pilot subcarriers are inserted since the channel is assumed to be perfectly known at the receiver. The multipath channel is assumed to be static during an OFDM symbol and consists of three taps. Without loss of generality, we assume that the channel taps are normalized such that $\sum_{l=0}^{L-1}\sigma^2_{h(l)} = 1$. A cyclic prefix of sufficient length is used in order to eliminate ISI. Figure 3 shows the average BER results for each of the three subcarrier groups discussed in Section 5 for 64 subcarriers. The theoretical average BER results are obtained using Eqs. (39), (45), and (52). The agreement between the theoretical and

Table 1 Simulation parameters

Parameter	Value
Number of subcarriers (N)	64, 256
Number of OFDM symbols simulated	4×10^6
Modulation scheme	BPSK
OFDM symbol duration	20 μs
Guard type and length	Cyclic prefix (16–64 subcarriers)
Channel delay	[0 1500 4000] μs
Channel gain	[0 −4 −8] dB

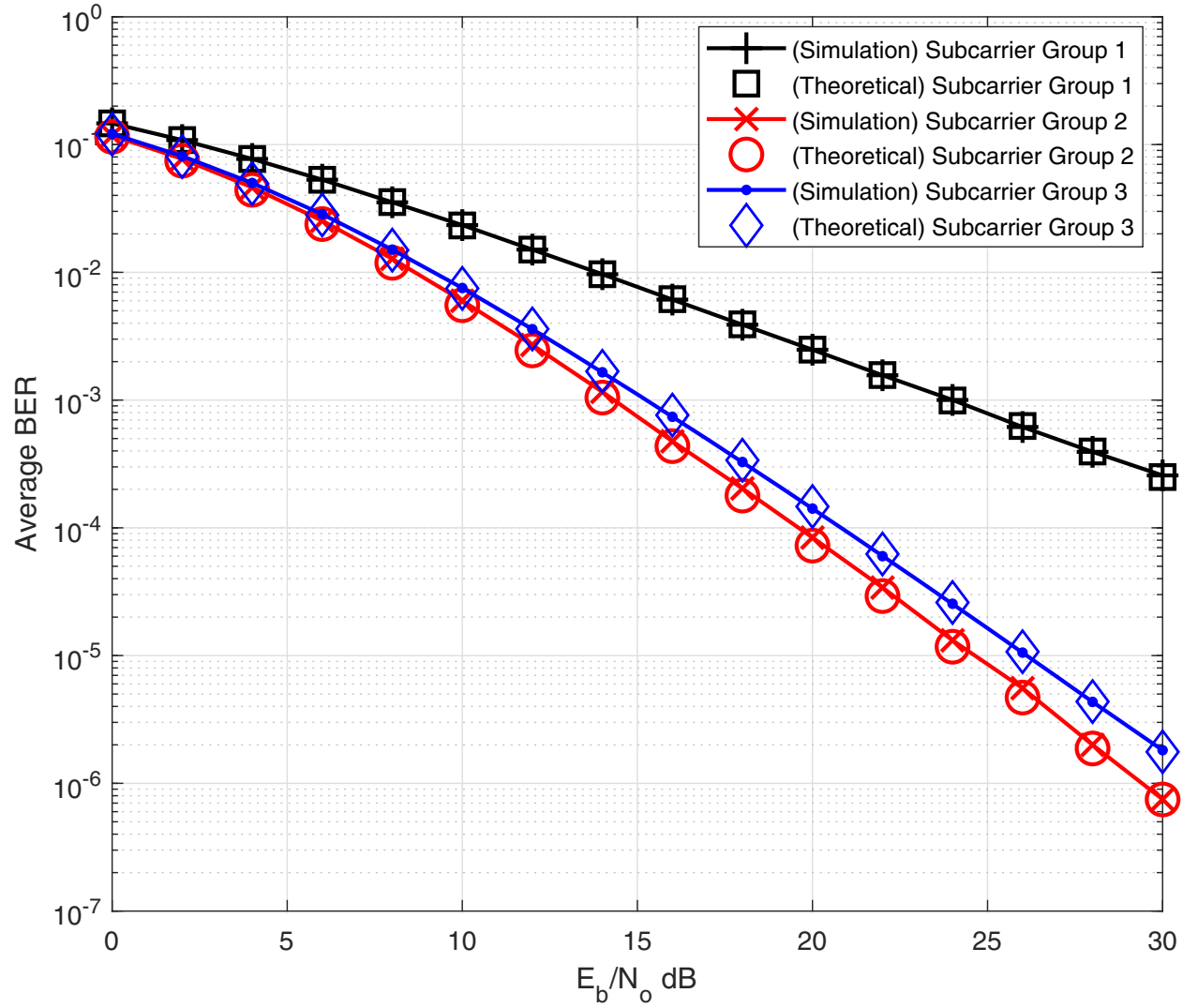

Fig. 3 Average BER vs. E_b/N_o for each subcarrier group assuming 64 subcarriers

simulation results is clear. Although subcarrier group 1 is shown to have the worst BER performance compared to the other two subcarrier groups, this group only contains two subcarriers of the N subcarriers constituting the OFDM symbol; hence, the impact of the performance of this group on the average BER of all subcarriers combined is expected to be minimal for large number of subcarriers N.

Next, we compare the performance of the proposed DHT-OFDM system with three other systems, namely, the conventional DFT-OFDM system [1], the generalized DHT-OFDM system [16], and the DHT-precoded OFDM system [22]. In the generalized DHT-OFDM system, the DFT is replaced by the DHT at the transmitter and receiver, and a transceiver scheme is proposed to diagonalize the channel matrix and eliminate the ICI at the receiver. The DHT-precoded OFDM system uses the DHT as a precoder to the conventional DFT-OFDM system. In the DHT-precoded OFDM system, the DHT is first applied to the modulated data stream before applying the IDFT on the output of the DHT. Because the combination of DHT and DFT will not result in a diagonal channel matrix, the authors in [22] proposed a new receiver scheme in which the channel equalization is performed between the DFT and the DHT blocks. This will not produce a diagonal matrix but rather a sparse matrix and hence, some ICI interference will be present at the receiver. Figure 4 shows the BER performance of the proposed DHT-OFDM system along with the conventional DFT-OFDM system, the generalized DHT-OFDM system, and the DHT-precoded OFDM system for 256 subcarriers. The proposed DHT-OFDM system

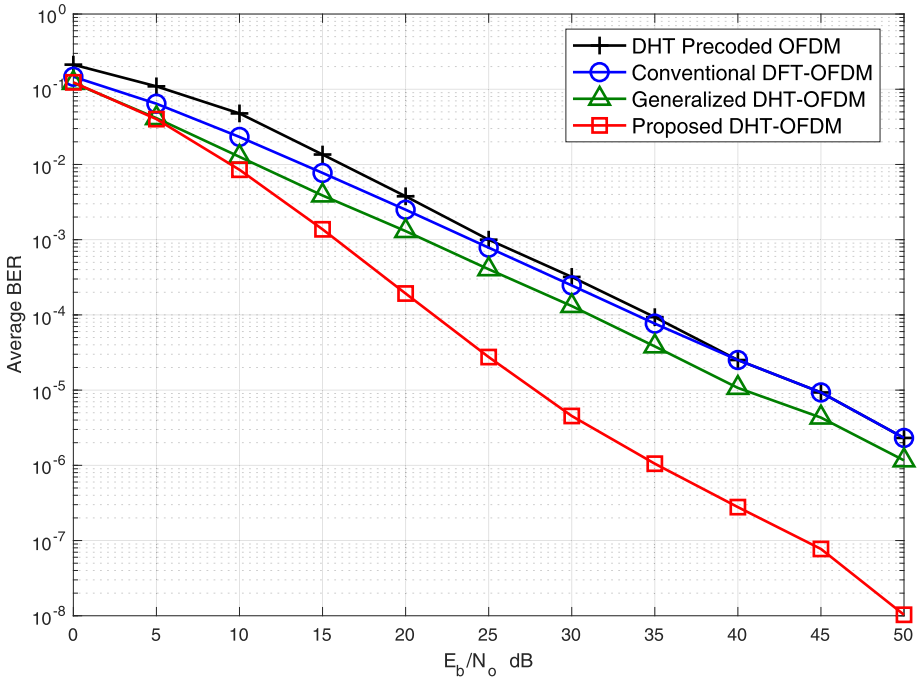

Fig. 4 Average BER vs. E_b/N_o comparison between the proposed DHT-OFDM system with the conventional DFT-OFDM, generalized DHT-OFDM, and the DHT-precoded OFDM systems (number of subcarriers = 256)

outperforms the conventional DFT-OFDM and the DHT-precoded OFDM systems by approximately 17 dB at an average BER of 10^{-5}, and outperforms the generalized DHT-OFDM by 12 dB at an average BER of 10^{-5}. The superior performance of the proposed system is due to the fact that rather than diagonalizing the channel matrix, the proposed system uses the coupling between subcarriers to increase the diversity gain and hence achieve better BER performance.

The performance of the proposed DHT-OFDM system under time-varying channel conditions is shown in Fig. 5 for 256 subcarriers. A mobile device is assumed to be moving at a speed of 120 km/h. At this speed, the Doppler frequency is measured to be 555.5 Hz. Although all systems experience an error floor at high signal-to-noise ratio values due to the ICI caused by the loss of orthogonality between subcarriers, the proposed DHT-OFDM system outperforms the other systems, and its error floor is introduced at substantially lower BER values.

Finally, the PAPR performance of the proposed DHT-OFDM is compared with the conventional DFT-OFDM system, the generalized DHT-OFDM system, and the DHT-precoded OFDM system. Figure 6 shows the complementary cumulative distribution function (CCDF) comparison of the proposed DHT-OFDM as well as the other three systems. The CCDF measures the probability that the PAPR exceeds some $PAPR_o$ level [30]. It can be seen in Fig. 6 that the proposed DHT-OFDM system suffers from an approximately 5.5, 2, and 1 dB increase in PAPR when compared to the DHT-precoded OFDM, the conventional DFT-OFDM, and the generalized DHT-OFDM systems, respectively. This is a minor trade-off when considering the large gains obtained in average BER as shown in Fig. 4.

8 Conclusions

In this paper, we considered using the DHT as an alternative to the conventional DFT in OFDM systems. When used, the DHT produces a uniquely structured channel matrix in which every two symmetric subcarriers are coupled together. Instead of treating the coupling between subcarriers as interference, we proposed a simple frequency-domain subcarrier diversity receiver to take advantage of the coupling between the subcarriers, and hence, reduce the average BER of the system by increasing the diversity gain between the coupled subcarriers. Detailed statistical and mathematical analyses of the system were provided, and a set of new closed-form expressions for the average BER of the proposed DHT-OFDM system are derived. Numerical results are shown to agree with the theoretical analysis. The proposed DHT-OFDM system outperforms the generalized DHT-OFDM system by 12 dB and outperforms the conventional DFT-OFDM and the DHT-precoded OFDM systems by 17 dB at an average BER of 10^{-5}. In terms of PAPR, the proposed system suffers from an approximately 5.5, 2, and 1 dB

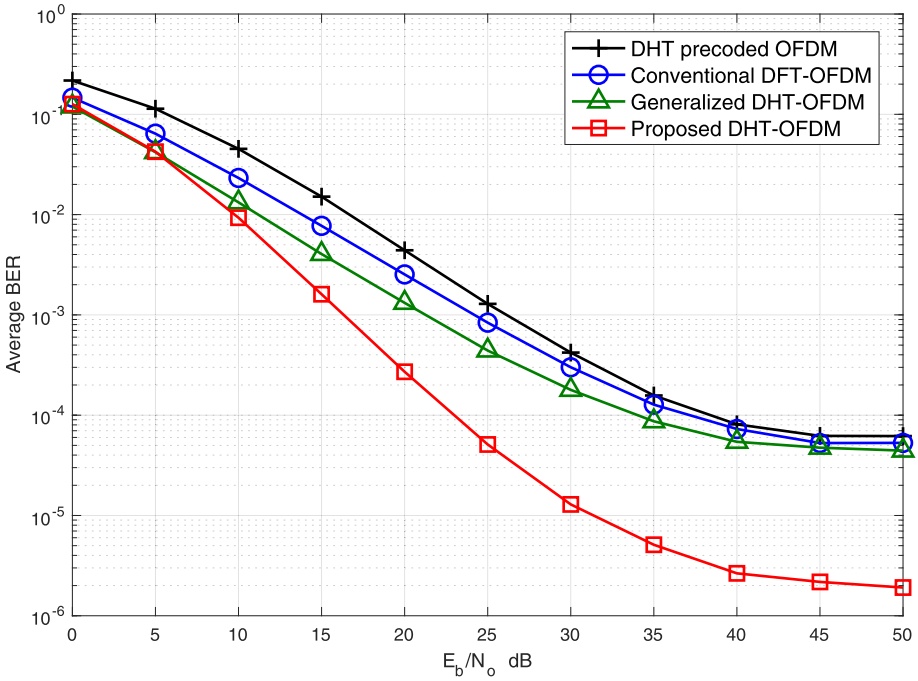

Fig. 5 Average BER vs. E_b/N_o comparison between the proposed DHT-OFDM system with the conventional DFT-OFDM, generalized DHT-OFDM, and the DHT-precoded OFDM systems at a speed of 120 km/h (number of subcarriers = 256)

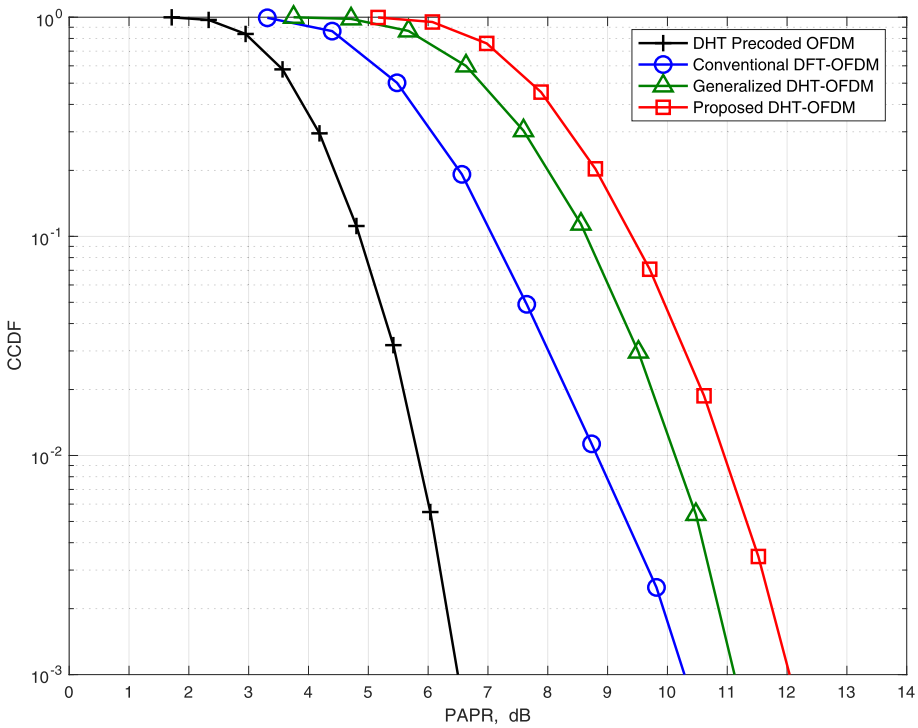

Fig. 6 PAPR performance comparison between the proposed DHT-OFDM with the conventional DFT-OFDM, generalized DHT-OFDM, and the DHT-precoded OFDM systems (number of subcarriers = 64)

increase in PAPR when compared to the DHT-precoded OFDM, the conventional DFT-OFDM, and the generalized DHT-OFDM system, respectively. This is a minor trade-off when considering the large gains obtained in average BER.

Abbreviations

BER: Bit error rate; BPSK: Binary phase shift keying; DFT: Discrete Fourier transform; CI: Coupling interference; DCT: Discrete cosine transform; DHT: Discrete Hartley transform; DST: Discrete sine transform; FFT: Fast Fourier transform; FPGA: Field-programmable gate arrays; ICI: Intercarrier interference; IDFT: Inverse discrete Fourier transform; IDHT: Inverse discrete Hartley transform; IFFT: Inverse fast Fourier transform; ISI: Intersymbol interference; OFDM: Orthogonal frequency-division multiplexing; PAPR: Peak-to-average power ratio; QAM: Quadrature amplitude modulation; WHT: Whalsh Hadamard transform; WPT: Wavelet packet transform; WSSUS: Wide sense stationary uncorrelated scattering

Funding

Not applicable.

Availability of data and materials

Not applicable.

Authors' contributions

MG is the main author of the current paper. MG contributed to the development of the ideas, design of the study, theory, result analysis, and article writing. AFA contributed to the development of the ideas, design of the study, the theory, simulation, result analysis, and article writing. All authors read and approved the final manuscript.

Authors' information

MG received his B.S. degree in electrical engineering from Kuwait University in 1998, and M.S. and Ph.D. degrees in electrical engineering from the University of California, San Diego in 2004 and 2007, respectively. Since 2007, he has been an assistant professor at the Electrical Engineering department in Kuwait University. AFA (S'91-M'00-SM' 07 of IEEE) received the B.S. degree in electrical engineering from the University of South Florida, Tampa, Florida, in 1993. He received M.S. and Ph.D. degrees in electrical engineering from the University of Florida, Gainesville, Florida, in 1995 and 2000, respectively. At the present, he is an associate professor at Electrical Engineering Department, Kuwait University and Vice Dean for Academic Affairs at the College of Engineering and Petroleum, Kuwait University. He served as the chairman of the Electrical Engineering Department, Kuwait University from March 2007 to September 2011.

Competing interests

The authors declare that they have no competing interests.

Publisher's Note

Received: 1 March 2018 Accepted: 10 March 2019
Published online: 28 March 2019

References

1. S. Weinstein, P. Ebert, Data transmission by frequency-division multiplexing using the discrete Fourier transform. IEEE Transactions on Communication Technology. **19**(5), 628–634 (1971)
2. M. Lehne, S. Raman, A discrete-time FFT processor for ultrawideband OFDM wireless transceivers: architecture and behavioral modeling. IEEE Trans. Circ. Syst. I Regular Paper. **57**(11), 3011–3022 (2010)
3. E. H. Krishna, K. Sivani, K. A. Reddy, in *IEEE International Conference on Computer and Computational Sciences: January 2015; Noida, India*. Hardware implementation of OFDM transceiver using FPGA, (2015), pp. 3–7
4. S.-C. Chen, C.-T. Yu, C.-L. Tsai, J.-J. Tang, in *IEEE Asia-Pacific Conference on Circuits and Systems: December 2004; Tainan, Taiwan*. A new IFFT/FFT hardware implementation structure for OFDM applications, (2004), pp. 1093–1096
5. A. Gangwar, M. Bhardwaj, An overview: peak to average power ratio in OFDM system and its effect. Int. J. Commun. Comput. Technol. **1**(2), 22–25 (2012)
6. B. Lim, Y. C. Ko, SIR analysis of OFDM and GFDM waveforms with timing offset, CFO and phase noise. IEEE Trans. Wirel. Commun. **16**(10), 6979–6990 (2017)
7. A. M. Hamza, J. W. Mark, Closed-form expressions for the BER/SER of OFDM systems with an integer time offset. IEEE Trans. Commun. **63**(11), 4461–4473 (2015)
8. M. Al-Gharabally, P. Das, in *IEEE International Conference on Communications: June 2006; Istanbul, Turkey*. On the Performance of OFDM Systems in Time Varying Channels with Channel Estimation Error, (2006), pp. 5180–5185
9. R. Merched, On OFDM and single-carrier frequency-domain systems based on trigonometric transforms. IEEE Signal Process. Lett. **13**(8), 473–476 (2006)
10. S. Shete, G. Bhide, M. Jadhav, in *IEEE International Conference on Advances in Electronics, Communication and Computer Technology: December 2016; Pune, India*. WHT and Double WHT: An effective PAPR reduction approach in OFDM, (2016), pp. 172–175
11. A. Li, W. Shieh, R. S. Tucker, Wavelet packet transform-based OFDM for optical communications. J. Light. Technol. **28**(24), 3519–3528 (2010)
12. C.-L. Wang, C.-H. Chang, J. L. Fan, J. M. Cioffi, in *Proceedings of the IEEE International Conference on Acoustics, Speech, and Signal Processing: June 2000; Istanbul*. Discrete Hartley transform based multicarrier modulation, (2000), pp. 2513–2516
13. M. S. Moreolo, Performance analysis of DHT-based optical OFDM using large-size constellations in AWGN. IEEE Commun. Lett. **15**(5), 572–574 (2011)
14. C. K. Jao, S. S. Long, M. T. Shiue, in *Proceedings of the IEEE 20th International Symposium on Personal, Indoor and Mobile Radio Communications: September 2009; Tokyo*. On the DHT-based multicarrier transceiver over multipath fading channel, (2009), pp. 1662–1666
15. P. S. Chen, C. K. Jao, M. T. Shiue, in *IEEE International Symposium on Circuits and Systems: May 2009; Taipei*. A low complexity real-valued kernel DHT-based OFDM modulator/demodulator design, (2009), pp. 1529–1532
16. C. K. Jao, S. S. Long, M. T. Shiue, DHT-based OFDM system for passband transmission over frequency-selective channel. IEEE Signal Process. Lett. **17**(8), 699–702 (2010)
17. Z. Wang, G. B. Giannakis, in *IEEE Third Workshop on Signal Processing Advances in Wireless Communications: March 2001; Taiwan, China*. Linearly Precoded or Coded OFDM against Wireless Channel Fades, (2001), pp. 267–270
18. X. Ouyang, J. Jin, G. Jin, P. Li, Low complexity discrete hartley transform precoded ofdm system over frequency selective fading channel. ETRI J. **37**(1), 32–42 (2001)
19. X. Ouyang, J. Jin, G. Jin, Z. Wang, in *Proceeding of the IEEE Wireless Communications and Networking Conference: April 2013; Shanghai*. Discrete Hartley transform based SFBC-OFDM transceiver design with low complexity, (2013), pp. 2744–2749
20. I. Baig, V. Jeoti, in *IEEE International Conference on Intelligent and Advanced Systems: June 2010: Kuala Lumpur*. PAPR analysis of DHT-precoded OFDM system for M-QAM, (2010), pp. 1–4
21. I. Baig, V. Jeoyi, A new discrete Hartley transform precoding based interleaved-OFDMA uplink system with reduced PAPR for 4G cellular networks. J. Eng. Sci. Technol. **6**(6), 685–694 (2011)
22. I. Ali, A. Pollok, L. Luo, L. Davis, in *IEEE 23rd International Symposium on Personal, Indoor and Mobile Radio Communications: September 2012; Sydney, Australia*. A DHT precoded OFDM system with full diversity and low PAPR, (2012), pp. 2383–2388
23. H. A. Leftah, S. Boussakta, in *IEEE International Conference on Communications: June 2013; Budapest*. Efficient modulation scheme for OFDM system with ZP and MMSE equalizer, (2013), pp. 4703–4707
24. V. Dimitrov, R. Baghaie, in *IEEE Conference Record of the Thirty-Third Asilomar Conference on Signals, Systems, and Computers: Oct. 1999*. Computing discrete Hartley transform using algebraic integers, (1999), pp. 1351–1355

25. A. D. Poularikas, *The Handbook of Formulas and Tables for Signal Processing*. (CRC Press, Boca Raton, 1999)
26. K.F. Tiampo, et al., Postseismic deformation following the 1994 Northridge earthquake identified using the localized Hartley transform filter. Pure Appl. Geophys. **165**(8), 1577–1602 (2008)
27. J. G. Proakis, *Digital Communications*. (McGraw Hill, United States, 2000)
28. H. Y. Kong, H. V. Khuong, D. H. Nam, Exact error and outage probability formulas for Alamouti space time code $2xj$. J. Commun. Netw. **9**(2), 177–184 (2007)
29. P. E. Oguntunde, O. A. Adetunmibi, A. O. Adejumo, On the sum of exponentially distributed random variables: a convolution approach. Eur. J. Stat. Probab. **1**(2), 1–8 (2013)
30. R. Ghahremani, M. G. Shayesteh, in *IEEE 22nd Iranian Conference on Electrical Engineering: May 2014; Tehran*. BER Performance Improvement and PAPR Reduction in OFDM Systems based on Combined DHT and μ -Law Companding, (2014), pp. 1483–1487